PERGAMON

International Journal of Heat and Mass Transfer 43 (2000) 2345–2363

International Journal of HEAT and MASS TRANSFER

www.elsevier.com/locate/ijhmt

Radiant and convective heat transfer on pneumatic transport of particles: an analytical study

Sávio Leandro Bertoli

Department of Chemical Engineering, Regional University of Blumenau, FURB, SC, C.P. 1507, 89010-971 Blumenau, Brazil

Received 29 October 1998; received in revised form 9 September 1999

Abstract

In this work, an analysis of the heat transfer to pneumatically conveyed oil shale fines particles is developed. A radiative–convective model, including radial dependence on the fluid temperature, is analytically solved by the use of the Laplace transform and modified Duhamel theorem [10]. It is demonstrated that the limiting case of infinity dilution of the particles results in the classical Graetz solution [15]. Results are analyzed and compared with experimental data and another existent lumped capacity solution [6]. © 2000 Elsevier Science Ltd. All rights reserved.

Keywords: Heat transfer on pneumatic transport; Gas–particle heat transfer; Heat exchange in moving beds; Radiative heat transfer in particulate flows; Heat transfer to gas–solid mixtures; Radiant and convective heat transfer in gaseous suspensions

1. Introduction

Physical and chemical processes, involving heat transfer to a flowing mixture of fluid and particles, have been industrially employed for a long time now. Catalyst regeneration, nuclear reactor cooling and oil shale pyrolisis are examples of these processes. Due to its technological importance, the phenomena have received wide treatment in the literature. Farbar and Morley [1] first demonstrated the possibility of increasing heat transfer rates by adding solid particles to a gaseous stream. Tien [2] obtained an analytical solution for the case of a turbulent mixture; however, his solution is restricted to a small Biot number ($Bi = h_p d_p/k_p$), solid/gas mass ratio less than 1 and absence of radiation. Matsumoto et al. [3] by means of the Laplace and Hankel transforms solved a model for small Biot numbers with no radiant heat transfer. Azad and Modest [4] developed a numerical analysis of the problem, considering radiation scattering. Their study is also limited to diluted suspensions and a small Biot number. An approximate solution considering radiant heat transfer and no restrictions in the particle Biot number was obtained by Lisbôa [5]. Bertoli [6], employing the Cauchy residue theorem, obtained the exact analytical solution of the Lisbôa model.

In this work, a two-phase, convective–radiative model (referred to in the text as distributed parameter model — DM), considering intraparticle temperature gradients and radial fluid temperature gradients, is analytically solved. The solution developed follows a different approach to that by Munro and Amudson [7], who employed the Laguerre theorem [8] to identify the character of the poles in the Laplace transform equations or that of Siegmund et al. [9], who used the finite Bessel transformation. The solution obtained will be employed to describe the oil shale fines pyrolysis

E-mail address: savio@furb.rct-sc.br (S.L. Bertoli).

0017-9310/00/$ - see front matter
PII: S0017-9310(99)00280-X

Nomenclature

A_w wall differential area, $= 2\pi R\,dx$
A_p surface area of single particle, $= \pi d_p^2$
d_p particle diameter
C specific heat at constant pressure
D_r pipe diameter
G mass flux
h_p fluid to particle heat transfer coefficient
h_w wall heat transfer coefficient
k thermal conductivity
L length of the heating section
n_v number of solid particles in the volume V
Pr Prandtl number, $= \frac{C_f \mu_f}{k_f}$
Nu_p Nusselt number, $= \frac{h_p d_p}{k_f}$
Q flow rate
r radial position in the tube
R pipe radius
Re Reynolds number, $= D_r \rho_f u_f / \mu_f$
Re_p particle Reynolds number, $= \rho_f d_p (u_{sf} - u_{tp})/\mu_f$
R_p particle radius
s Laplace variable
T temperature
T_{fi} fluid inlet temperature
T_{pi} particle inlet temperature
T_{ps} particle surface temperature
T_w wall temperature
u axial velocity
u_{sf} superficial gas velocity
u_{tp} terminal particle velocity
V pipe differential volume $= \pi R^2\,dx$
W_s solid feed rate
x axial distance

Greek symbols
α thermal diffusivity
Δ $= \varphi + \gamma$
ε void fraction
ε_p surface emissivity of particles
γ $= \frac{n_v h_p A_p}{V \rho_f C_f}$
μ dynamic viscosity
ξ radial position inside a particle
ρ density
σ Stefan–Boltzmann constant
φ $= h_w A_w / V \rho_f C_f$

Subscripts
f fluid
p particle

process. The influence of design parameters, such as wall temperature, mass flux ratio, and Reynolds number on the mean temperature of the fluid and the particles, and also on the Nusselt number and convective, as well as radiant heat fluxes, are determined. The results are compared with experimental data from the literature [5] and with another lumped capacity solution [6] that considers the uniform fluid temperature throughout the pipe cross-section.

2. Analysis

The main restrictions of this study are the following:

- the heat absorbed by the chemical reaction (the pyrolysis of oil shale is an endothermic reaction) is negligible in comparison with the overall demand of the process;
- the pipe wall is isothermal (T_w = const.) and black;
- the particles are gray; the gas is transparent to radiation; the configuration factor from the particle to the wall is 1;
- the flow is developed in the two-phase system and the velocity profiles for the fluid and the particles are uniform throughout the pipe cross-section. The particles and fluid may have different velocities;
- the particles are spheres of uniform size and are uniformly distributed over the pipe cross section;
- the physical properties are uniform and constant;
- the eddy thermal diffusivity of the fluid is negligible;
- the amount of heat exchanged by convection between the fluid and the particles is independent of the radial position in the tube;
- the radiative heat transfer in the axial direction is neglected when compared with the radial radiative heat transfer.

3. Governing equations

Considering the above restrictions and defining t as the particle residence time

$$t = \frac{x}{u_p} \tag{1}$$

an energy balance in the spherical coordinate system yields the particle temperature equation:

$$\frac{1}{\alpha_p}\frac{\partial T_p(\xi, t)}{\partial t} = \frac{\partial^2 T_p(\xi, t)}{\partial \xi^2} + \frac{2}{\xi}\frac{\partial T_p(\xi, t)}{\partial \xi} \tag{2}$$

Similarly, an energy balance in the cylindrical coordinate system yields the fluid temperature equation :

$$\frac{\rho_f c_f u_f}{u_p}\frac{\partial T_f}{\partial t} = \frac{n_v h_p A_p}{V}\left(T_{ps} - \bar{T}_f\right) + \frac{1}{r}\frac{\partial}{\partial r}\left(r k_f \frac{\partial T_f}{\partial r}\right)$$

$$T_f = T_f(r, t)$$

$$T_{ps} = T_{ps}(t) \tag{3}$$

$\bar{T}_f(t)$ is the mean radial fluid temperature in time t, given by:

$$\bar{T}_f(t) = \frac{2}{R^2}\int_0^R T_f(r, t) r \, dr \tag{4}$$

The system formed by Eqs. (2)–(4) is subjected to the following initial and boundary conditions:

$$r = R: \qquad T_f = T_w \tag{5}$$

$$r = 0: \qquad T_f = \text{finite} \tag{6}$$

$$t = 0: \qquad T_f = T_{fi} \tag{7}$$

$$\xi = R_p,\ t > 0: \qquad T_p = T_{ps}(t) \tag{8}$$

$$\xi = 0,\ t > 0: \qquad T_p = \text{finite} \tag{9}$$

$$t = 0,\ 0 < \xi < R_p: \qquad T_p = T_{pi} \tag{10}$$

and also the additional condition:

$$\xi = R_p,\ t > 0:$$
$$-k_p\frac{\partial T_p}{\partial \xi} = h_p\left(T_{ps}(t) - \bar{T}_f\right) + h_r\left(T_{ps}(t) - T_w\right) \tag{11}$$

In the above equation, n_v/V is the number of particles per unit volume:

$$\frac{n_v}{V} = \frac{6W_s}{\rho_p \pi^2 d_p^3 u_p R^2} \tag{12}$$

and h_r is the radiant heat transfer coefficient between the wall and the particle, given by:

$$h_r = \varepsilon_p \sigma\left(T_w^2 + T_{ps}^2\right)\left(T_w + T_{ps}\right) \tag{13}$$

4. Solution of the model in the Laplace domain

To solve Eqs. (1)–(11), we initially define:

$$\chi = \frac{u_f}{u_p} \tag{14}$$

and make the following variable change:

$$\theta_p(\xi, t) = \frac{T_p(\xi, t) - T_{pi}}{T_{pi}}. \tag{15}$$

Then, rewriting the equations for the particle and fluid, we have:

$$\frac{1}{\alpha_p}\frac{\partial \theta_p}{\partial t} = \frac{2}{\xi}\frac{\partial \theta_p}{\partial \xi} + \frac{\partial^2 \theta_p}{\partial \xi^2} \tag{16}$$

$$\chi\frac{\partial T_f}{\partial t} = \gamma\left(T_{ps} - \bar{T}_f\right) + \alpha\left(\frac{1}{r}\frac{\partial T_f}{\partial r} + \frac{\partial^2 T_f}{\partial r^2}\right) \tag{17}$$

The boundary and additional conditions are also:

$$\xi = R_p,\ t > 0: \qquad \theta_p = \frac{T_{ps}(t) - T_{pi}}{T_{pi}} \equiv \phi(t) \tag{18}$$

$$\xi = 0,\ t > 0: \qquad \theta_p = \text{finite} \tag{19}$$

$$t = 0,\ 0 < \xi < R_p: \qquad \theta_p = 0 \tag{20}$$

$$\xi = R_p,\ t > 0:$$
$$\frac{\partial \theta_p}{\partial \xi} = -\frac{h_p}{k_p}\left[\phi(t) + \frac{T_{pi} - \bar{T}_f(t)}{T_{pi}}\right] - \frac{h_r}{k_p}\left[\phi(t) + \frac{T_{pi} - T_w}{T_{pi}}\right] \tag{21}$$

The solution of this coupled system of equations is obtained in the Laplace domain. The subsequent development, results in the transformed equations.

According to the work of Hackenberg [10], the problem described by Eq. (16) and conditions (18)–(20) has the following solution:

$$\theta_p(\xi, t) = \int_0^t u(\xi, t - \tau)\frac{\partial \phi(\tau)}{\partial \tau}\, d\tau + \phi(0)u(\xi, r), \tag{22}$$

where $u(\xi, t)$ is the solution of the auxiliary problem:

$$\frac{\partial^2 u(\xi, t)}{\partial \xi^2} + \frac{2}{\xi}\frac{\partial u(\xi, t)}{\partial \xi} = \frac{1}{\alpha_p}\frac{\partial u(\xi, t)}{\partial t} \tag{23}$$

$$\text{B.C.1:} \quad \xi = 0,\ t > 0: \qquad u = \text{finite} \tag{24}$$

$$\text{B.C.2:}\ \xi = R_p,\ t > 0: \qquad u = 1 \tag{25}$$

$$\text{I.C.:}\ 0 < \xi < R_p,\ t = 0: \qquad u = 0 \tag{26}$$

and in given by

$$u(\xi, t) = 1 + \frac{2R_p}{\pi\xi}\sum_{j=1}^{\infty}\frac{(-1)^j}{j}\sin\left(\frac{j\pi\xi}{R_p}\right) \times \exp\left[-\left(\frac{j\pi}{R_p}\right)^2\alpha_p t\right] \tag{27}$$

Taking the first derivative of θ_p (expressed by Eq. (22)) in ξ and substituting the auxiliary condition, we can determine $\phi(t)$:

$$\frac{\partial\phi(t)}{\partial t} * \left.\frac{\partial u(\xi, t)}{\partial\xi}\right|_{\xi=R_p} + \phi(0)\frac{\partial u(\xi, t)}{\partial\xi} = G(t), \tag{28}$$

where (*) is the convolution operation and $G(t)$ is given by:

$$G(t) = -\frac{h_p}{k_p}\left[\phi(t) + \frac{T_{pi} - \bar{T}_f(t)}{T_{pi}}\right] - \frac{h_r}{k_p}\left[\phi(t) + \frac{T_{pi} - T_w}{T_{ps}}\right] \tag{29}$$

Substituting Eq. (27) into Eq. (28), we have:

$$\frac{\partial\phi(t)}{\partial t} * \frac{2}{R_p}K_1^{\infty}(t) + \phi(0)\frac{2}{R_p}K_1^{\infty}(t) = G(t), \tag{30}$$

where

$$K_1^{\infty}(t) = \sum_{j=1}^{\infty}\exp\left[-\frac{j^2\pi^2\alpha_p t}{R_p^2}\right] \tag{31}$$

Developing Eq. (30), results:

$$\frac{2}{R_p}\int_0^1\phi'(\tau)K_1^{\infty}(t-\tau)\,d\tau + \frac{2}{R_p}\phi(0)K_1^{\infty}(t) = -\frac{h_p + h_r}{k_p}\phi(t) + \frac{h_p}{k_p}\left(\frac{T_f(t) - T_{pi}}{T_{pi}}\right) + \frac{h_r}{k_p}\left(\frac{T_w - T_{pi}}{T_{pi}}\right) \tag{32}$$

Multiplying the above equation by $k_p/(h_p + h_r)$ and defining,

$$\delta = \frac{2k_p}{R_p(h_p + h_r)} \tag{33}$$

$$\omega = \frac{h_p}{h_p + h_r} \tag{34}$$

$$\eta = \frac{h_p}{h_p + h_r}\frac{T_w - T_{pi}}{T_{pi}} \tag{35}$$

and,

$$f(t) = \omega\frac{T_f(t) - T_{pi}}{T_{pi}} + \eta \tag{36}$$

Then we may write Eq. (32) as,

$$\delta\int_0^t\phi'(\tau)K_1^{\infty}(t-\tau)\,d\tau + \delta\phi(0)K_1^{\infty}(t) = -\phi(t) + f(t) \tag{37}$$

Applying the Laplace transform to this equation, after some manipulation, we obtain:

$$\phi(s) = \frac{f(s)}{1 + \delta s K_1^{\infty}(s)} \tag{38}$$

where,

$$K_1^{\infty}(s) = \sum_{j=1}^{\infty}\frac{1}{s + \pi^2\alpha_p j^2/R_p^2} \tag{39}$$

or, in terms of hyperbolic functions [11],

$$K_1^{\infty}(s) = \frac{R_p^2}{\alpha_p}\left[\frac{\coth(y)}{2y} - \frac{1}{2y^2}\right] \tag{40}$$

and,

$$y = R_p\sqrt{\frac{s}{\alpha_p}} \tag{41}$$

$f(s)$ is obtained from Eq. (36) and $\phi(s)$ from Eq. (18):

$$f(s) = \omega\frac{\bar{T}_f(s)}{T_{pi}} - \frac{1}{s}(\omega - \eta) \tag{42}$$

$$\phi(s) = \frac{T_{ps}(s)}{T_{pi}} - \frac{1}{s} \tag{43}$$

Substituting Eqs. (39), (42) and (43) into Eq. (38) and isolating $T_{ps}(s)$, we finally have,

$$T_{ps}(s) = \frac{2\omega\bar{T}_f(s)}{2 + \delta\big(y\coth(y) - 1\big)} + \frac{T_{pi}}{s}\left[1 - \frac{2(\omega - \eta)}{2 + \delta\big(y\coth(y) - 1\big)}\right] \tag{44}$$

The equation for the fluid temperature in the Laplace domain is directly obtained from Eq. (17) and the initial condition:

$$\chi\left(sT_{\mathrm{f}}(r,s)-T_{\mathrm{fi}}\right)$$

$$=\gamma\left(T_{\mathrm{ps}}(s)-\bar{T}_{\mathrm{f}}(s)\right)+\frac{\alpha}{r}\frac{\mathrm{d}T_{\mathrm{f}}(r,s)}{\mathrm{d}r}+\alpha\frac{\mathrm{d}^2T_{\mathrm{f}}(r,s)}{\mathrm{d}r^2}$$

Rearranging the above equation, follows:

$$\frac{\mathrm{d}^2T_{\mathrm{f}}(r,s)}{\mathrm{d}r^2}+\frac{1}{r}\frac{\mathrm{d}T_{\mathrm{f}}(r,s)}{\mathrm{d}r}-\frac{\chi s}{\alpha}T_{\mathrm{f}}(r,s)$$

$$=\frac{\gamma}{\alpha}\left(\bar{T}_{\mathrm{f}}(s)-T_{\mathrm{ps}}(s)\right)-\frac{\chi T_{\mathrm{fi}}}{\alpha} \tag{45}$$

The solution of this inhomogeneous equation is given by:

$$T_{\mathrm{f}}(r,s)=T_{\mathrm{fh}}+T_{\mathrm{fp}},$$

where T_{fh} is the solution of the associated homogeneous, and T_{fp} is a particular solution.

4.1. Solution of the homogenous equation

$$r^2\frac{\mathrm{d}^2T_{\mathrm{fh}}}{\mathrm{d}r^2}+r\frac{\mathrm{d}T_{\mathrm{fh}}}{\mathrm{d}r}-\frac{s\chi}{\alpha}r^2T_{\mathrm{fh}}=0 \tag{46}$$

The above equation is a modified Bessel equation of zero order, with a parameter $s\chi/\alpha$, of the solution

$$T_{\mathrm{fh}}=A\,I_0(\lambda r)+B\,K_0(\lambda r). \tag{47}$$

A and B are constants to be determined and $I_0(\lambda r)$ and $K_0(\lambda r)$ are Bessel modified functions of the first and second kind and zero order, respectively, and λ is given by:

$$\lambda=\sqrt{s\chi/\alpha^2} \tag{48}$$

4.2. Particular solution

From Eq. (45) we determine the following particular solution:

$$T_{\mathrm{fp}}=-\beta(s) \tag{49}$$

where we find

$$\beta(s)=\frac{\gamma}{\chi s}\left(\bar{T}_{\mathrm{f}}(s)-T_{\mathrm{ps}}(s)\right)-\frac{T_{\mathrm{fi}}}{s} \tag{50}$$

4.3. General solution

Adding Eqs. (47) and (49) results the general solution of Eq. (45):

$$T_{\mathrm{f}}(r,s)=A\,I_0(\lambda r)+B\,K_0(\lambda r)-\beta(s) \tag{51}$$

Also, according to the boundary condition at $r=0$ (Eq. (6)), T_{f} is limited, then $B=0$ ($K_0(\lambda r)$ is unbounded at $r=0$ [12]). Substituting B and the Laplace transform of Eq. (5) into Eq. (51), follows:

$$T_{\mathrm{f}}(R,s)=\frac{T_{\mathrm{w}}}{s}=A\,I_0(\lambda R)-\beta(s)$$

Therefore,

$$A=\frac{T_{\mathrm{w}}/s+\beta(s)}{I_0(\lambda r)},$$

With the above constants, the solution for $T_{\mathrm{f}}(r,s)$ is:

$$T_{\mathrm{f}}(r,s)=T_{\mathrm{w}}\frac{I_0(\lambda r)}{s\,I_0(\lambda R)}+\beta(s)\left(\frac{I_0(\lambda r)}{I_0(\lambda R)}-1\right) \tag{52}$$

The Laplace transform for $\bar{T}_{\mathrm{f}}(t)$ is obtained from Eq. (4):

$$\bar{T}_{\mathrm{f}}(s)=\frac{2}{R^2}\int_0^R T_{\mathrm{f}}(r,s)r\,\mathrm{d}r \tag{53}$$

Carrying Eq. (52) to the above integral, we get:

$$\bar{T}_{\mathrm{f}}(s)=\frac{2}{R^2\,I_0(\lambda R)}\left[\frac{T_{\mathrm{w}}}{s}+\beta(s)\right]\int_0^R I_0(\lambda r)r\,\mathrm{d}r-\beta(s)$$

From the integrals of Bessel functions [13], we have:

$$\int_0^R \lambda r\,I_0(\lambda r)\,\mathrm{d}(\lambda r)=\lambda R I_1(\lambda R).$$

Then,

$$\bar{T}_{\mathrm{f}}(s)=\frac{2I_1(\lambda R)}{\lambda R I_0(\lambda R)}\left[\frac{T_{\mathrm{w}}}{s}+\beta(s)\right]-\beta(s), \tag{54}$$

from the recurrence relations of Bessel functions [12] we have:

$$\lambda R I_2(\lambda R)=\lambda R\,I_0(\lambda R)-2I_1(\lambda R) \tag{55}$$

Rearranging Eq. (54) and substituting Eq. (55),

$$\bar{T}_{\mathrm{f}}(s)=\frac{2T_{\mathrm{w}}}{\lambda R s}\frac{I_1(\lambda R)}{I_0(\lambda R)}-\beta(s)\frac{I_2(\lambda R)}{I_0(\lambda R)} \tag{56}$$

By substituting Eq. (44) into Eq. (50), we eliminate T_{ps} in the expression of $\beta(s)$:

$$\beta(s)=-\gamma\left[p(s)\bar{T}_{\mathrm{f}}(s)+\frac{h(s)T_{\mathrm{pi}}}{s}\right]-\frac{T_{\mathrm{fi}}}{s}, \tag{57}$$

where we obtain

$$p(s)=\frac{1}{\chi s}\left\{\frac{2\omega}{2+\delta\left[y\coth(y)-1\right]}-1\right\} \tag{58}$$

$$h(s)=\frac{1}{\chi s}\left\{1-\frac{2(\omega-\eta)}{2+\delta\left[y\coth(y)-1\right]}\right\} \tag{59}$$

Finally, carrying Eq. (57) to Eq. (58), results:

$$\bar{T}_{\mathrm{f}}(s)=\frac{2T_{\mathrm{w}}I_1(\lambda R)+\left(\gamma h(s)T_{\mathrm{pi}}+T_{\mathrm{fi}}\right)\lambda RI_2(\lambda R)}{\left(I_0(\lambda R)-\gamma p(s)I_2(\lambda R)\right)s\lambda R}s\lambda R \tag{60}$$

Now, expressing Eqs. (44) and (52) in terms of $p(s)$ and $h(s)$, we conclude the solution of the system in Laplace domain:

$$T_{\mathrm{ps}}(s)=\left(\chi sp(s)+1\right)\bar{T}_{\mathrm{f}}(s)+\chi T_{\mathrm{pi}}h(s) \tag{61}$$

$$T_{\mathrm{f}}(r,s)=\frac{T_{\mathrm{w}}}{s}\frac{I_0(\lambda r)}{I_0(\lambda R)}-\left(\gamma p(s)\bar{T}_{\mathrm{f}}(s)+\frac{T_{\mathrm{fi}}}{s}+\gamma\frac{h(s)}{s}T_{\mathrm{pi}}\right)\left[\frac{I_0(\lambda r)}{I_0(\lambda R)}-1\right] \tag{62}$$

5. Inversion of the Laplace transforms

The inverse Laplace transforms of Eqs. (52), (60) and (61) is obtained by the Cauchy Residue theorem. Following this method, the inverse Laplace transform of the function $f(s)$ is given by [14]: $L^{-1}[f(s)]=\sum$ Residues of $f(s)\mathrm{e}^{st}$. The summation is evaluated over the poles of $f(s)\mathrm{e}^{st}$. The residue of the pole b of $g(s)$ can be obtained by: $\mathrm{Res}(b)=\frac{1}{(m-1)!}\lim_{s\to b}\frac{\mathrm{d}^{m-1}}{\mathrm{d}s^{m-1}}[(s-b)^m g(s)]$, where m is the order of the pole.

Due to the lengthy development in the evaluation of the residues, we refer ourselves to another work [6] in the details; here we present the resulting residues at each pole.

5.1. Inversion of $T_{\mathrm{f}}(r,s)$

To make it easier, we separate $T_{\mathrm{f}}(r,s)\mathrm{e}^{st}$ in two parts:

$$A_1(r,s)=\frac{T_{\mathrm{w}}}{s}\frac{I_0(\lambda r)}{I_0(\lambda R)}\mathrm{e}^{st} \tag{63}$$

and

$$A_2(r,s)=\beta(s)\left[\frac{I_0(\lambda r)}{I_0(\lambda R)}-1\right]\mathrm{e}^{st}, \tag{64}$$

Now, the character and residue of poles will be determined.

5.1.1. Character of poles of $A_1(r,s)$

Eqs. (63) and (48) reveals that $A_1(r,s)$ have first-order poles at $s=0$ and $s=-\alpha\rho_n^2/\chi$, where $\pm\rho_n$, $n=1,2,\ldots$ are the roots of

$$J_0(\rho R)=0 \tag{65}$$

The residues are [6]:

$$\mathrm{Res}(0)=T_{\mathrm{w}} \tag{66}$$

$$\mathrm{Res}\left(-\alpha\rho_n^2/\chi\right)=-\frac{2T_{\mathrm{w}}}{R}\sum_{n=1}^{\infty}\frac{\exp\left(-\alpha\rho_n^2/\chi\right)}{\rho_n}\frac{J_0(\rho_n r)}{J_1(\rho_n R)} \tag{67}$$

5.1.2. Character of poles of $A_2(r,s)$

From Appendix A, $A_2(r,s)$ have first-order poles at $s=-\alpha_{\mathrm{p}}\nu_n^2$, $s=-\alpha\tau_n^2/\chi$, $s=-\alpha\rho_n^2/\chi$ and a second-order pole at $s=0$ where $\pm\rho_n$, $n=1,2,\ldots$ are the roots of Eq. (65), $\pm\nu_n$, $n=1,2,\ldots$ are the roots of:

$$2+\delta\left[\nu R_{\mathrm{p}}\cot\left(\nu R_{\mathrm{p}}\right)-1\right]=0 \tag{68}$$

and $\pm\tau_n$, $n=1,2,\ldots$ are the roots of:

$$J_0(\tau R)+\gamma p\left(-\alpha\tau^2/\chi\right)J_2(\tau R)=0 \tag{69}$$

The residues are [6]:

$$\mathrm{Res}\left(-\alpha_{\mathrm{p}}\nu_n^2\right)=0 \tag{70}$$

$$\mathrm{Res}\left(-\alpha\rho_n^2/\chi\right)=\frac{4T_{\mathrm{w}}}{R^2}\sum_{n=1}^{\infty}\frac{\exp\left(-\alpha\rho_n^2 t/\chi\right)}{\rho_n^2}\frac{J_0(\rho_n r)}{J_2(\rho_n R)} \tag{71}$$

$$\mathrm{Res}(0)=0 \tag{72}$$

$$\mathrm{Res}(a_n)=4\gamma\sum_{n=1}^{\infty}\mathrm{e}^{a_n t}\left[\frac{J_0(\tau_n r)}{J_0(\tau_n R)}-1\right]\times\frac{\left\{T_{\mathrm{w}}-T_{\mathrm{fi}}-\gamma\left[h(a_n)T_{\mathrm{pi}}+p(a_n)T_{\mathrm{w}}\right]\right\}p(a_n)}{(\tau_n R)^2\left[1-\gamma p(a_n)\right]^2+4\gamma\left[p(a_n)-a_n p'(a_n)\right]} \tag{73}$$

where:

$$p(a_n)=\frac{1}{\chi a_n}\left\{\frac{2\omega}{2+\delta\left[D|a_n|^{1/2}\cot\left(D|a_n|^{1/2}\right)-1\right]}-1\right\} \tag{74}$$

$$h(a_n)=\frac{1}{\chi a_n}\left\{1-\frac{2(\omega-\eta)}{2+\delta\left[D|a_n|^{1/2}\cot\left(D|a_n|^{1/2}\right)-1\right]}\right\} \tag{75}$$

$$p'(a_n) = \frac{-p(a_n)}{a_n} - \frac{\omega\delta D}{\chi a_n |a_n|^{1/2}} \times \left\{ \frac{D|a_n|^{1/2}\left[1+\cot^2\left(D|a_n|^{1/2}\right)\right] - \cot\left(D|a_n|^{1/2}\right)}{\left\{2+\delta\left[D|a_n|^{1/2}\cot\left(D|a_n|^{1/2}\right)-1\right]\right\}^2} \right\} \tag{76}$$

$$a_n = -\alpha\tau_n^2/\chi \tag{77}$$

and,

$$D = \frac{R_p}{\alpha_p^{1/2}} \tag{78}$$

The inverse of $T_f(r, s)$ is obtained by combining Eqs. (65)–(67) and (70)–(73); the resulting expression is:

$$T_f(r,t) = T_w + 4\gamma\sum_{n=1}^{\infty} e^{a_n t}\left[\frac{J_0(\tau_n r)}{J_0(\tau_n R)} - 1\right] \times \frac{\left\{T_w - T_{fi} - \gamma\left[h(a_n)T_{pi} + p(a_n)T_w\right]\right\}p(a_n)}{(\tau_n R)^2\left[1-\gamma p(a_n)\right]^2 + 4\gamma\left[p(a_n) - a_n p'(a_n)\right]} \tag{79}$$

The functions $p(a_n), p'(a_n)$ and $h(a_n)$ are defined by Eqs. (74)–(76); a_n is given by Eq. (77).

5.2. Inversion of $T_{ps}(s)$

From Appendix A, $T_{ps}(s)$ have first-order poles at $s = -\alpha_p\nu_n^2$, $s = -\alpha\tau_n^2/\chi$ and $s = 0$; where $\pm\nu_n$ and $\pm\tau_n$, $n = 1, 2, \ldots$ are the roots of Eqs. (68) and (69), respectively. The residues are [6]:

$$\mathrm{Res}\left(-\alpha_p\nu_n^2\right) = 0 \tag{80}$$

$$\mathrm{Res}(0) = T_w \tag{81}$$

$$\mathrm{Res}\left(-\alpha\tau_n^2/\chi\right) = -4\omega\sum_{n=1}^{\infty} e^{a_n t} r(a_n) \times \frac{T_w - T_{fi} - \gamma\left[h(a_n)T_{pi} + p(a_n)T_w\right]}{(\tau_{nR})^2\left[1-\gamma p(a_n)\right]^2 + 4\gamma\left[p(a_n) - a_n p'(a_n)\right]} \tag{82}$$

$$r(a_n) = \frac{2}{2+\delta\left[D|a_n|^{1/2}\cot\left(D|a_n|^{1/2}\right)-1\right]} \tag{83}$$

Finally, summing Eqs. (80)–(82), results in the inverse of $T_{ps}(s)$:

$$T_{ps}(t) = T_w - 4\omega\sum_{n=1}^{\infty} e^{a_n t} r(a_n) \times \frac{T_w - T_{fi} - \gamma\left[h(a_n)T_{pi} + p(a_n)T_w\right]}{(\tau_n R)^2\left[1-\gamma p(a_n)\right]^2 + 4\gamma\left[p(a_n) - a_n p'(a_n)\right]} \tag{84}$$

The functions $p(a_n)$, $h(a_n)$, $p'(a_n)$ and $r(a_n)$ are defined by Eqs. (74)–(76), and (83), respectively.

Now, defining the following function,

$$F(a_n) = \frac{T_w - T_{fi} - \gamma\left[h(a_n)T_{pi} + p(a_n)T_w\right]}{(\tau_n R)^2\left[1-\gamma p(a_n)\right]^2 + 4\gamma\left[p(a_n) - a_n p'(a_n)\right]} \tag{85}$$

we can put the equations for the fluid and particle surface temperature in the form:

$$T_f(r,t) = T_w + 4\gamma\sum_{n=1}^{\infty} e^{a_n t}\left[\frac{J_0(\tau_n r)}{J_0(\tau_n R)} - 1\right]p(a_n)F(a_n) \tag{86}$$

$$T_{ps}(t) = T_w - 4\omega\sum_{n=1}^{\infty} e^{a_n t} r(a_n)F(a_n), \tag{87}$$

From the following equation:

$$\phi(t) = \frac{T_{ps}(t) - T_{pi}}{T_{pi}},$$

we obtain $\theta_p(\xi, t)$ by Eq. (22),

$$\phi_p(\xi,t) = \int_0^t \left\{1 + \frac{2R_p}{\pi\xi}\sum_{j=1}^{\infty}\frac{(-1)^j}{j}\sin\left(\frac{j\pi\xi}{R_p}\right) \times \exp\left[-\left(\frac{j\pi}{R_p}\right)^2\alpha_p(t-\tau)\right]\right\} \times \frac{\partial\phi(\tau)}{\partial\tau}d\tau + \phi(0)\left\{1 + \frac{2R_p}{\pi\xi}\sum_{j=1}^{\infty}\frac{(-1)^j}{j} \times \sin\left(\frac{j\pi\xi}{R_p}\right)\exp\left[-\left(\frac{j\pi}{R_p}\right)^2\alpha_p t\right]\right\} \tag{88}$$

Introducing $\phi(t)$ into the equation above and developing it results:

$$\theta_p(\xi, t) = \phi(t) + \frac{2R_p}{\pi\xi}\sum_{j=1}^{\infty}\frac{(-1)^j}{j}\sin\left(\frac{j\pi\xi}{R_p}\right)\left\{\phi(0) \times \exp\left[-\left(\frac{j\pi}{R_p}\right)^2\alpha_p t\right] - \frac{4\omega}{T_{pi}}\sum_{n=1}^{\infty}\left\{\exp(a_n t) - \exp\left[-\left(\frac{j\pi}{R_p}\right)^2\alpha_p t\right]\right\}\frac{a_n r(a_n)F(a_n)}{a_n + \alpha_p\left(j\pi/R_p\right)^2}\right\} \quad (89)$$

Substituting the expression of $\theta_p(\xi, t)$ (Eq. (15)), we find

$$T_p(\xi, t) = \phi(t)T_{pi} + \frac{2R_p}{\pi\xi}\sum_{j=1}^{\infty}\frac{(-1)^j}{j}\sin\left(\frac{j\pi\xi}{R_p}\right) \times \left\{\phi(0)T_{pi}\exp\left[-\left(\frac{j\pi}{R_p}\right)^2\alpha_p t\right] - 4\omega \times \sum_{n=1}^{\infty}\left\{\exp(a_n t) - \exp\left[-\left(\frac{j\pi}{R_p}\right)^2\alpha_p t\right]\right\} \times \frac{a_n r(a_n)F(a_n)}{a_n + \alpha_p\left(j\pi/R_p\right)^2}\right\} + T_{pi} \quad (90)$$

The temperature at the center of the particle is obtained from the above equation by a limit process:

$$T_p(0, t) = \phi(t)T_{pi} + 2\sum_{j=1}^{\infty}(-1)^j \times \left\{\phi(0)T_{pi}\exp\left[-\left(\frac{j\pi}{R_p}\right)^2\alpha_p t\right] - 4\omega\sum_{n=1}^{\infty}\left\{\exp(a_n t) - \exp\left[-\left(\frac{j\pi}{R_p}\right)^2\alpha_p t\right]\right\} \times \frac{a_n r(a_n)F(a_n)}{a_n + \alpha_p\left(j\pi/R_p\right)^2}\right\} + T_{pi} \quad (91)$$

The mean temperature of the particle is given by:

$$\bar{T}_p(t) = \frac{4\pi}{V_p}\int_0^{R_p} T_p(\xi, t)\xi^2\,d\xi \quad (92)$$

Now, substituting Eq. (90) in this equation and integrating, results:

$$\bar{T}_p(t) = \phi(t)T_{pi} - \frac{6}{\pi^2}\sum_{j=1}^{\infty}\frac{1}{j^2} \times \left\{\phi(0)T_{pi}\exp\left[-\left(\frac{j\pi}{R_p}\right)^2\alpha_p t\right] - 4\omega\sum_{n=1}^{\infty}\left\{\exp(a_n t) - \exp\left[-\left(\frac{j\pi}{R_p}\right)^2\alpha_p t\right]\right\} \times \frac{a_n r(a_n)F(a_n)}{a_n + \alpha_p\left(j\pi/R_p\right)^2}\right\} + T_{pi} \quad (93)$$

Carrying Eq. (79) to Eq. (4), we obtain the mean temperature of the fluid at time t:

$$\bar{T}_f(t) = T_w + 4\gamma\sum_{n=1}^{\infty}e^{a_n t}F(a_n)p(a_n)\frac{2}{R^2} \int_0^R\left[\frac{J_0(\tau_n r)}{J_0(\tau_n R)} - 1\right]r\,dr \quad (94)$$

From the integrals of the Bessel functions [13],

$$\int_0^R J_0(\tau_n r)r\,dr = \frac{R}{\tau_n}J_1(\tau_n R) \quad (95)$$

therefore,

$$\frac{2}{R^2}\int_0^R\left[\frac{J_0(\tau_n r)}{J_0(\tau_n R)} - 1\right]r\,dr = \frac{2J_1(\tau_n R)}{\tau_n R J_0(\tau_n R)} - 1 \quad (96)$$

From [12] we have the following relation:

$$2J_1(\tau_n R) = \tau_n R\left[J_2(\tau_n R) + J_0(\tau_n R)\right] \quad (97)$$

Combining Eqs. (69), (96) and (97) results in the value of the integral:

$$\frac{2}{R^2}\int_0^R\left[\frac{J_0(\tau_n r)}{J_0(\tau_n R)} - 1\right]r\,dr = -\frac{1}{\gamma p(a_n)}$$

Finally, carrying this result to Eq. (94), we have:

$$\bar{T}_f(t) = T_w - 4\sum_{n=1}^{\infty}e^{a_n t}F(a_n) \quad (98)$$

where a_n is given by Eq. (77).

6. Results and discussion

One of the major drawbacks in employing the Cauchy residue theorem in the inversion of Laplace transforms arises when the character of the poles is not easily determined. In fact, other works [7] have found some difficulties in the inversion of transformed equations. In such a case, the Laguerre theorem [8]

was employed to establish the character of some poles. However, this theorem says nothing about the zero multiplicity that is necessary to evaluate the order of poles. Strictly speaking, the character of zeros of the expression, $I_0(\lambda R) - \gamma p(s) I_2(\lambda R)$ that appears in the denominator of $\bar{T}_f(s)$, Eq. (60), cannot be established by the Laguerre theorem. In the present analysis, we made a development (see Appendix A) that possibly overcomes these difficulties, extending the use of the Laplace transforms and Cauchy Residue theorem to this class of problems.

Now, by Eq. (69),

$$\gamma p(a_n) = \frac{-J_0(\tau_n R)}{J_2(\tau_n R)},$$

substituting this result in Eq. (86),

$$T_f(r, t) = T_w - 4\sum_{n=1}^{\infty}\left[\frac{J_0(\tau_n r)}{J_0(\tau_n R)} - 1\right]\frac{J_0(\tau_n R)}{J_2(\tau_n R)} F(a_n) e^{a_n t} \tag{99}$$

in case of a pure fluid, $\gamma \to 0$; then by Eq. (69),

$$J_0(\tau_n R) = 0$$

or $\tau_n \to \rho_n \quad n = 1, 2, 3 \ldots$

by Eq. (85),

$$\lim_{\gamma \to 0} F(a_n) = \frac{(T_w - T_{fi})}{(\rho_n R)^2},$$

also, when $\gamma \to 0$, $u_p \to u_f$ and consequently $\chi \to 1$. Substituting the above results in Eq. (99), follows

$$\lim_{\gamma \to 0} T_f(r, t) = T_w + 4(T_{fi} - T_w) \times \sum_{n=1}^{\infty}\left[\frac{J_0(\rho_n r)}{(\rho_n R)^2 J_2(\rho_n R)} e^{-\alpha \rho_n^2 t}\right] \tag{100}$$

then by Eqs. (97) and (65),

$$2J_1(\rho_n R) = \rho_n R J_2(\rho_n R)$$

Carrying this result to Eq. (100) we finally obtain:

$$T_f(r, t) = T_w + 2(T_{fi} - T_w)\sum_{n=1}^{\infty}\left[\frac{J_0(\rho_n r)}{\rho_n R J_1(\rho_n R)} e^{-\alpha \rho_n^2 t}\right] \tag{101}$$

which is the classical Graetz solution [15] for the heating of a fluid in a duct of uniform velocity over the cross section.

Although a great part of this study deals with the development of analytical solution of the proposed model, we will in the following paragraphs discuss some features relative to it.

The assumption, that the temperature distribution of the particles is uniform over the tube cross section, is equivalent to considering that the solid eddy diffusivity of heat, $\varepsilon_{H,P}$, is extremely large (at convection dominant conditions). Due to the fact that we have neglected the eddy thermal diffusivity of the fluid, $\varepsilon_{H,f}$, this means that there is no correlation between $\varepsilon_{H,P}$ and $\varepsilon_{H,f}$. The assumption of radial independence in the heat exchanged between the fluid and particles may cause some distortion in the fluid temperature profile, which is minimized in systems with high thermal diffusivity of the fluid or high simultaneous particle–wall radiative and fluid–particle convective heat transfer (in the case of fluid transparent to radiation), since in this case, the fluid temperature profile tends to be more uniform over the tube cross section.

The calculated values of the heat fluxes and the fluid, and the particle temperatures will be presented in the following. The predictions of the model are compared with a series of thermal tests realized by Lisbôa [5] in an experimental unit with a mixture of oil shale fines particles and air, and also with an existent lumped capacity model [6] described in Appendix B for completeness. The experimental apparatus used is described in Lisbôa's work in detail [5]. In brief, the apparatus is a vertical pressure type transport system. The test section consists of a 20.9 mm I.D.,1 m long iron tube and its wall temperature was maintained by electric resistance. Gas (air) temperatures in the tube were measured at the inlet and outlet of the heating section by thermocouples. The particle temperature at the outlet of the heating section was determined indirectly by means of a thermal balance. The conditions and results of this tests are reproduced in Tables 1 and 2. In Table 1, the fluid and particle velocities and the bed porosity are theoretical values obtained by the solution of a hydrodynamical model. In Table 2, the fluid–particle heat transfer coefficient is obtained from Kato's correlation [16]:

$$Nu_p = 2.38 \times 10^{-3}(Re_p)^n \left[\frac{\varepsilon}{1-\varepsilon}\right]^{0.97} \tag{102}$$

with

$$n = 2.48\left(\frac{\varepsilon}{1-\varepsilon}\right)^{-0.28} \tag{103}$$

In accordance with the work of Lisbôa [5], this correlation gives the best agreement with the tests conditions. The wall–mixture heat transfer coefficient required by the lumped capacity solution (see Appendix B) is given by the following equation, obtained in the experimental unit [5]:

Table 1
Conditions of the tests realized by Lisbôa [5]

Test No.	W_s (kg/h)	$\frac{W_s}{W_f}$	u_f (m/s)	u_p (m/s)	ε
01	22.6	2.9	5.164	2.650	0.9970
02	50.0	6.4	5.182	2.684	0.9935
03	24.7	3.2	5.165	2.652	0.9968
04	52.2	6.7	5.183	2.686	0.9932
05	21.0	2.7	5.162	2.649	0.9972
06	44.0	5.6	5.178	2.677	0.9943

$$h_w = \frac{k_f}{D} 0.015 Re^{0.8}\, Pr^{0.4} \tag{104}$$

Both correlations are adopted in the present analysis. The physical oil shale fines properties and the particle mean diameter are also obtained from Lisbôa [5]:

- thermal conductivity, $k_p = 1.4$ W/m °C;
- density, $\rho_p = 2.30$ g/cm^3;
- specific heat, $C_p = 961.4$ J/kg °C;
- emissivity, $\varepsilon_p = 0.86$;
- particle mean diameter, $d_p = 348.8$ μm (Sauter mass basis).

In the simulations with the model, the gas properties (air) were calculated iteratively at the mean temperature in the pipe. Table 3 presents a comparison between the results of distributed parameter solution (DP) and a previous lumped capacity solution (LP) [6] with the experimental data obtained by Lisbôa [5] with a mixture of oil shale fines particles and air. We observe that the predictions of both models compare well with the experimental data. Also, Table 4 presents the calculated temperatures at the particle surface (Eq. (84)) and at the center of the particle (Eq. (91)) for $L = 1$ m at the tests conditions. Although the temperature differences are low, the results have shown that intraparticle temperature gradients of 6900 K/m (test 5) were found.

The figures that follow relate a dependent variable (e.g. Nusselt number) with an independent variable (e.g. L/D_T) for the hydrodynamical conditions listed in Table 5.

Fig. 1 presents the influence of wall temperature in the mean temperature of the fluid for the cases of a solid/gas mass ratio (W_s/W_f) of 2.7 and 7.8 as predicted by the present solution (DP) and the lumped parameter solution (LP) [6] (see Appendix B). Fig. 2 shows results for the mean temperature of particles under the same conditions. It demonstrates a good agreement between the solutions of both models. As expected, $\bar{T}_f$ and $\bar{T}p$ increase with increasing T_w. With W_s/W_f increasing, $\bar{T}_f$ and $\bar{T}p$ diminish as a consequence of the greater heat capacity of the mixture.

Defining the total, radiant and convective heat fluxes at the wall respectively:

$$(q_T)_w = (q_R)_w + (q_C)_w \tag{105}$$

$$(q_R)_w = h_r \frac{n_v A_p}{A_w} \left(T_w - T_{ps}(t)\right) \tag{106}$$

$$(q_C)_w = -k_f \left.\frac{\partial T_f}{\partial r}\right|_{r=R} \tag{107}$$

with h_r given by Eq. (13), then from Eqs. (86), (69) and the derivatives of Bessel functions [12], we have:

$$(q_C)_w = -2Rk_f \sum_{n=1}^{\infty} e^{a_n t} \tau_n^2 \left\{\gamma p(a_n) - 1\right\} F(a_n) \tag{108}$$

Fig. 3 presents the influence of wall temperature

Table 2
Conditions and results of the tests realized by Lisbôa [5] (the heating section is a 0.75 in Sch 40 tube, $L = 1$ m)

Test No.	T_w (°C)	T_{fi} (°C)	T_{pi} (°C)	h_w (W/m^2 °C)	h_p (W/m^2 °C)	$T_f(L)$ (°C)	$T_p(L)$ (°C)
01	200.0	32.0	32.0	19.20	367.7	68.5	64.2
02	200.0	28.0	28.0	19.36	274.2	60.1	49.8
03	300.0	32.7	32.7	19.04	361.2	92.8	78.3
04	300.0	32.8	32.8	19.17	271.6	86.0	65.1
05	400.0	28.0	28.0	18.87	387.2	125.5	97.5
06	400.0	31.0	31.0	18.99	289.0	106.0	80.3

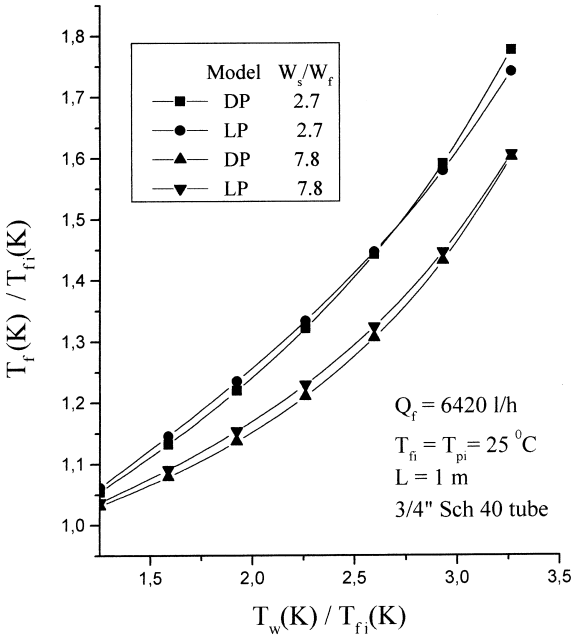

Fig. 1. Comparison between DP and LP [6] solutions for the mean temperature of fluid.

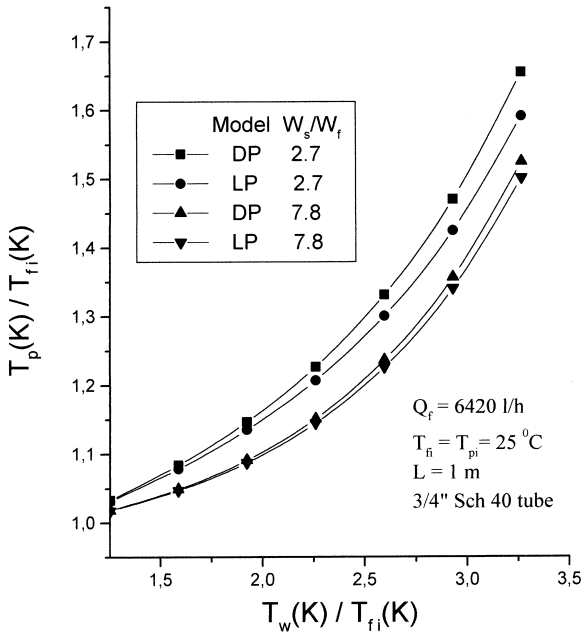

Fig. 2. Comparison between DP and LP [6] solutions for the mean particle temperature.

Table 3
Comparison between lumped parameter (LP) [6] and distributed parameter (DP) solutions and experimental data [5]

Test No.	Distributed parameter (DP)				Lumped parameter (LP) [6]			
	$\bar{T}_f(L)$ (°C)	$\Delta Tr_{,f}$ [a]	$\bar{T}_p(L)$ (°C)	$\Delta Tr_{,p}$ [b]	$\bar{T}_f(L)$ (°C)	$\Delta Tr_{,f}$	$\bar{T}_p(L)$ (°C)	$\Delta Tr_{,p}$
1	69.36	1.024	55.51	0.730	73.01	1.124	54.01	0.683
2	55.02	0.842	44.32	0.748	58.50	0.950	43.51	0.711
3	92.53	0.996	72.74	0.878	97.94	1.085	70.36	0.826
4	77.24	0.835	62.07	0.906	82.30	0.930	60.76	0.866
5	122.46	0.969	95.57	0.972	130.21	1.048	92.14	0.923
6	103.43	0.966	82.29	1.040	110.67	1.062	80.36	1.001

[a] $\Delta Tr_{,f} = (T_f, \text{calc.} - T_{fi})/(T_f, \text{exp.} - T_{fi})$..
[b] $\Delta Tr_{,p} = (T_p, \text{calc.} - T_{pi})/(T_p, \text{exp.} - T_{pi})$..

Table 4
Calculated temperatures at the particle surface and at the center of the particle for conditions of thermal tests at $L = 1$ m

Test No.	1	2	3	4	5	6
$T_{ps}(L)$ (°C)	55.68	44.44	73.03	62.29	96.05	82.67
$T_p(0, L)$ (°C)	55.24	44.14	72.30	61.75	94.84	81.72

Table 5
Hydrodynamical conditions employed in the analysis of the thermal model

Q_f (l/h)	W_s (kg/h)	$\frac{W_s}{W_f}$	u_f (m/s)	u_p (m/s)	ε
6.420	21.0	2.7	5.162	2.649	0.9972
6.420	44.0	5.6	5.178	2.677	0.9943
6.420	64.7	7.8	5.192	2.699	0.9916

and solid/gas mass ratio in the relative radiant heat flux at the wall $(q_R)_w/(q_T)_w$. We observe that both factors promote the relative radiant heat flux (note that in the present model, $(q_R)_w \sim W_s T^4/u_p$ and $(q_C)_w \sim T$).

For the particle surface, the total, radiant and convective heat fluxes are given by:

$$(q_T)_{ps} = (q_R)_{ps} + (q_C)_{ps} \tag{109}$$

$$(q_R)_{ps} = h_r\left(T_w - T_{ps}(t)\right) \tag{110}$$

$$(q_C)_{ps} = h_p\left(\bar{T}_f(t) - T_{ps}(t)\right) \tag{111}$$

Fig. 4 shows the influence of T_w and W_s/W_f in the radiant relative heat flux at the particle surface $(q_R)_{ps}/(q_T)_{ps}$. It is interesting to note that for $T_w = 300°C$ ($W_s/W_f = 2.7$) the radiant heat flux represents 30–48% of the total heat flux at the particle surface, in contrast with the fact that normally at this wall temperature, radiant effects are disregarded.

However, the following factors that were not included in the model equations, can substantially diminish the radiant flux for the mixture:

- Heat loss at the tube inlet and outlet; Eq. (13) assumes a dilute particulate bed. At the tube inlet and outlet, the configuration factor from the particle to the wall will be lower than 1. Therefore, in the tubes where the ratio D_r/L is high, this solution will predict values of temperatures higher than the real ones (for the experimental unit of Table 1, $D_r/L = 0.02093$).
- Interruption of the radiant flux to a determined par-

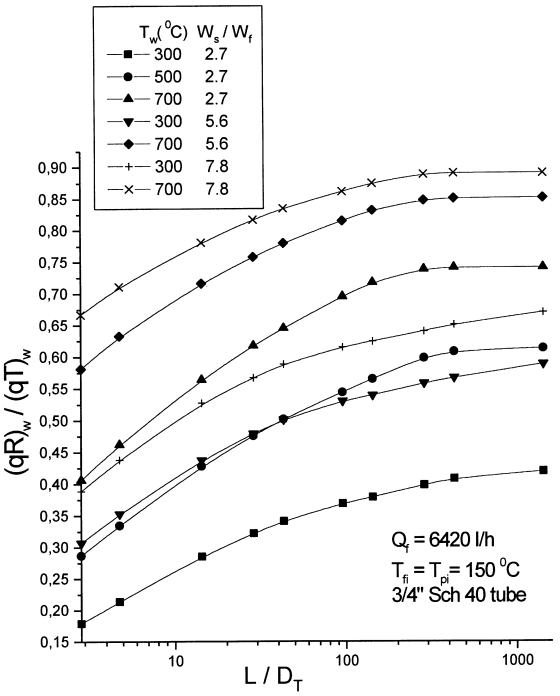

Fig. 3. Influence of the wall temperature and the loading ratio on the relative radiant heat flux at the wall.

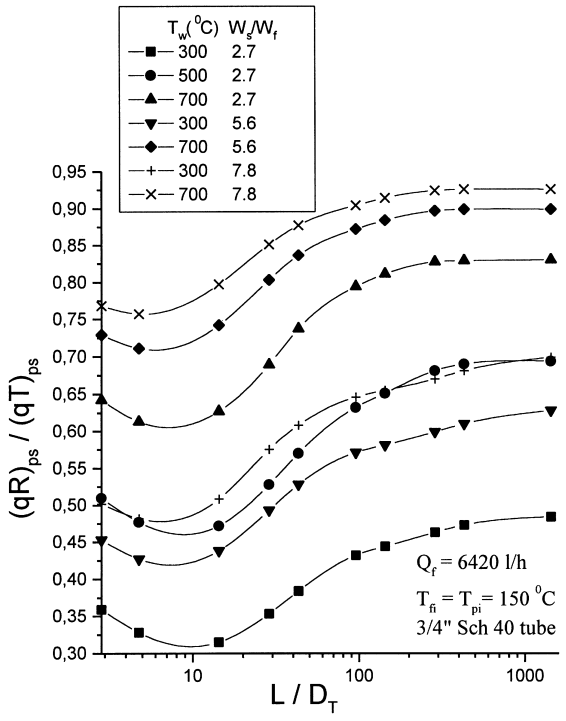

Fig. 4. Influence of the wall temperature and the loading ratio on the relative radiant heat flux at the particle surface.

ticle due to the presence of other particles (blinding);
- Radiation scattering.

The blinding effect also decreases the configuration factor from the particle to the wall, resulting in lower radiant coefficients, h_r. The scattering effect will be discussed later.The increase in the relative radiant flux at the particle surface for increasing loading ratios is explained by the decrease in the bed porosity which results in smaller values of h_p [16] (see Tables 1 and 2), and consequently in smaller $(q_C)_{ps}$.

The minimum relative radiant flux that appears in Fig. 4 corresponds approximately to the point of the greatest convective heat transfer between the fluid and particle. First, due to the greater heat capacity of the solids in comparison with the heat capacity of the fluid, the ratio $(q_R)_{ps}/(q_T)_{ps}$ decreases with L until a minimum (i.e., $h_p(\bar{T}_f(t) - T_{ps}(t))$ increases faster than $h_r(T_w - T_{ps}(t))$). After the minimum, the increase in $T_{ps}(t)$ and consequently in h_r (see Eq. (13)) counterbalances the increase in $\bar{T}_f(t)$, resulting in an increase of the ratio $(q_R)_{ps}/(q_T)_{ps}$. The local Nusselt number at the reactor length L is defined as:

$$Nu_L^T = \frac{2h_L R}{k_f} = \frac{2R(q_T)_w}{k_f(T_w - T_{mm})} \tag{112}$$

or,

$$Nu_L^T = Nu_L^C + Nu_L^R \tag{113}$$

where,

$$Nu_L^C = \frac{2R(q_C)_w}{k_f(T_w - T_{mm})} \tag{114}$$

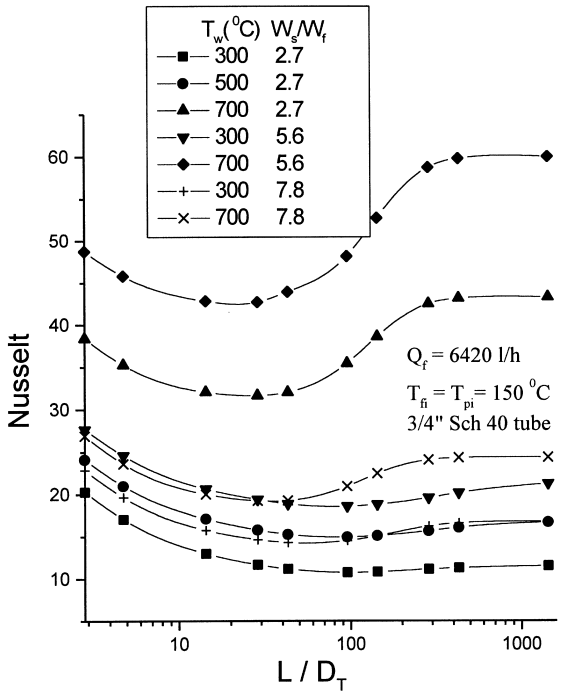

Fig. 5. Influence of the wall temperature and the loading ratio on the local Nusselt number.

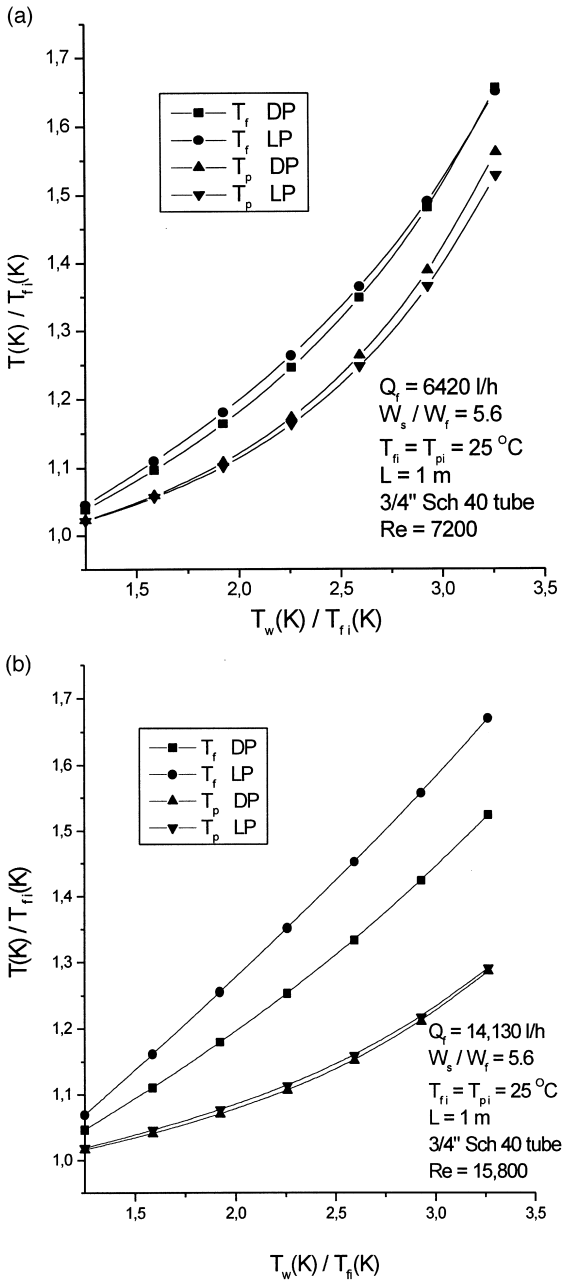

Fig. 6. Comparison between the results of LP [6] and DP solutions at (a) $Re = 7200$ and (b) $Re = 15{,}800$.

$$Nu_L^R = \frac{2R(q_R)_w}{k_f(T_w - T_{mm})} \quad (115)$$

T_{mm} is the mixed mean temperature as defined by Boothroyd and Haque [17]:

$$T_{mm} = \frac{W_f C_f \bar{T}_f + W_s C_p \bar{T}_p}{W_f C_f + W_s C_p} \quad (116)$$

Fig. 5 shows the influence of W_s/W_f and T_w on the local Nusselt number. In the same manner that $(q_R)_w/(q_T)_w$ (Fig. 3), the increase in these factors causes an increase in the Nusselt number. The minimum that appears in the curves of these figure was also observed by Tamehiro et al. [18] and Azad and Modest [4]. The minimum Nusselt number being a more conservative value is interesting to design.

The main differences between the heat fluxes predicted by the present solution and the lumped capacity solution [6] are observed at small values of the heating section, L. These differences are due to the fact that in the distributed parameter model (present work) the wall to mixture coefficient, h_w, is a local coefficient. At greater values of the heating section, the two solutions present similar results since h_w tends to the mean coefficient, $\bar{h}_w$ [6].

Fig. 6(a) and (b) depict a comparison between the lumped capacity solution [6] and the present one for the mean temperatures of the fluid and particles, respectively, as a function of the wall temperature and at different Reynolds numbers ($Re = D_r G_f/\mu_f$ at the heating section entrance). As the Reynolds number varies from 7200 to 15,800, it is possible to verify that the values of $\bar{T}_f$ predicted by the LP solution [6], are greater than the DP solution; this result was expected since in the DP model the turbulent thermal diffusivity of the fluid was assumed negligible.

In the present analysis, the scattering of radiation by the particles was not considered, however it will be demonstrated that it occurs. According to the description in the Handbook of Heat Transfer Fundamentals [19], for large particles the scattering criterion is:

$$\frac{\pi d_p}{\lambda} \gg 1$$

where λ is the radiation wavelength which may be calculated by Wien's law:

$$\lambda = \frac{2884\ \mu m\ K}{T\,(K)}$$

In Lisbôa's [5] experiment $d_p \approx 3.5 \times 10^{-4}$ m and $T_w \approx 700$ K, therefore, $\lambda \approx 4$ μm and $\pi d_p/\lambda \approx 275 \gg 1$ → geometrical scattering. Also, according to Brewster and Tien [20], the scattering is type independent. The importance of this scattering depends on the phase function and the scattering albedo. But, as described in [19], large particles are forward scattering in general; in this case the scattered energy behaves similar to transmitting radiation, reducing the influence of scattering [4] (it is important to note that despite the restrictions that the particles have spherical shape, oil shale particles are flake-like). As a final consideration, we note that the last simplifying assumption has been shown to be a good approximation except for regions close to a temperature jump [21].

7. Conclusions

The analytical methods employed in this work made it possible to obtain an analytical solution to the problem of radiant and convective heat transfer to a pneumatically conveyed mixture of particles, including radial dependence on fluid temperature. The main difficulties related to the determination of the character of the poles were overcome by the method described in Appendix A. For infinity dilution ($\gamma \to 0$) the solution obtained results in the classical Graetz [15] solution for the case of the fluid flowing alone. The comparison with experimental data available in the literature demonstrated that the present solution describes well the fluid and particle temperatures in the heating of a pneumatically conveyed mixture of oil shale fines particles and air. It must be pointed out, however, that the experimental data is available only for low wall temperatures (up to 400°C) and the oil shale process pyrolisis is normally conducted at $T_w \approx 700$°C. It should also be desirable to compare the results over a broader range of hydrodynamic conditions. At moderate Reynolds numbers, the results of the present model agree well with an existent lumped capacity solution [6]. The main advantage in this case is the fact that it is not necessary to employ a correlation for the wall–mixture heat transfer coefficient, since it can be determined from the temperature profile. The solution obtained obviously can be applied to other processes involving heat transfer to a gas–solid mixture, pneumatically conveyed, provided the assumptions that were made, apply. Particularly, one must avoid systems with low bed porosity and high wall temperatures where strong blinding effects can occur. For systems with a large particle Biot number no other analytical solution, which includes radiation, are available, so far as we know (except the approximate solution of Lisbôa [5]); so, the present model can be employed.

Finally, it must be remembered that the accuracy of the thermal model will depend on adequate correlations for the heat transfer coefficient h_p and a good hydrodynamic model.

Acknowledgements

To my wife Regiane for her help in writing the English version of this manuscript.

This work is in memory of Prof. Cirus Macedo Hackenberg.

Appendix A. Character of poles of $A_2(r, s)$, Eq. (64)

Substituting Eqs. (58) and (59) into Eqs. (57) and (60) it follows that,

$$\bar{T}_f(s) = \left\{ 2T_w I_1(\lambda R) + \left[\frac{\gamma}{\chi s}\left[1 - \frac{2(\omega-\eta)}{2+\delta\left[y\coth(y)-1\right]} \right] T_{pi} + T_{fi} \right] \times \lambda R I_2(\lambda R) \right\} \times \left\{ \left[I_0(\lambda R) - \frac{\gamma}{\chi s} \times \left[\frac{2\omega}{2+\delta\left[y\coth(y)-1\right]} - 1 \right] I_2(\lambda R) \right] s\,\lambda R \right\}^{-1} \quad \text{(A1)}$$

$$\beta(s) = -\frac{\gamma}{\chi s}\left[\frac{2\omega}{2+\delta\left[y\coth(y)-1\right]} - 1 \right] \bar{T}_f(s) - \frac{\gamma}{\chi s^2}\left[1 - \frac{2(\omega-\eta)}{2+\delta\left[y\coth(y)-1\right]} \right] T_{pi} - \frac{T_{fi}}{s} \quad \text{(A2)}$$

From Eqs. (64), (A1), (A2) and by the definition of $p(s)$, Eq. (58), $A_2(r, s)$ is analytic except at $s = 0$, $s = -\alpha\rho_n^2/\chi$, $n = 1, 2, \ldots$ ($\pm\rho_n$ are the roots of Eq. (65) $\Rightarrow s = -\alpha\rho_n^2/\chi$ is a first-order pole) and at the roots of:

$$2 + \delta\left(y\coth(y) - 1\right) = 0 \quad \text{(A3)}$$

and

$$I_0(\lambda R) - \gamma p(s) I_2(\lambda R) = 0 \quad \text{(A4)}$$

where λ is defined by Eq. (48). From the equations listed above, $s = 0$ will be a second-order pole except if it is a root of multiplicity greater than 1 in Eq. (A4). This will be verified in the following:

1. Roots of Eq. (A3): Employing Eqs. (39) and (40) we rewrite Eq. (A3) in the form:

$$1 + \delta s \sum_{j=1}^{\infty} \frac{1}{s + zj^2} = 0 \quad \text{(A5)}$$

where

$$z = \pi^2\alpha_p/R_p^2,$$

also, by Eq. (33), δ is a real positive constant

First case: $s \in R_+ \Rightarrow$ Eq. (A5), will have no roots, since

$$1 + \delta s \sum_{j=1}^{\infty} \frac{1}{s + zj^2} \geq 1, \quad \forall s \geq 0$$

Second case: $s \in R_-^*$; let $s = -a$, $a > 0$; then Eq. (A5) becomes:

$$1 - \delta a \sum_{j=1}^{\infty} \frac{1}{zj^2 - a} = 0$$

This equation has one root in the interval

$$zj^2 < a < z(j+1)^2 \quad j = 0, 1, 2, 3 \ldots$$

once the equation varies from 1 to $-\infty$ in the first interval and from $+\infty$ to $-\infty$ in the others.
Third case: $s \in I_+$; let $s = bi$, $b > 0$; then from Eq. (A5),

$$1 + \delta bi \sum_{j=1}^{\infty} \frac{1}{bi + zj^2} = 0$$

taking the product by the complex conjugate in the series, results

$$1 + \delta b \sum_{j=1}^{\infty} \frac{b + zj^2 i}{b^2 + \left(zj^2\right)^2} = 0$$

The above equation reveals that both imaginary and real terms are positive, therefore, it has no roots of type $s = bi$.
Fourth case: $s \in I_-$; in this case, a similar analysis as above leads to the same conclusion: There are no roots like $s = -bi$.
Fifth case: $s \in C$, $\ni$ $s = a - bi$; rearranging Eq. (A5),

$$\sum_{j=1}^{\infty} \frac{s}{s + zj^2} = -\frac{1}{\delta} \quad \text{(A6)}$$

Now, for $s = a - bi$,

$$\sum_{j=1}^{\infty} \frac{a - bi}{a - bi + zj^2} = -\frac{1}{\delta}$$

taking the product by the complex conjugate in the above equation and developing, it follows that,

$$\sum_{j=1}^{\infty}\frac{a\left(a+zj^2\right)+b^2-zj^2 i}{\left(a+zj^2\right)^2+b^2}=-\frac{1}{\delta}$$

The above equation reveals that it is impossible to cancel the imaginary (or real) terms, so, for $s \in C,\ \ni\ s=a-bi \Rightarrow \nexists$ roots for Eq. (A5).
Sixth case: $s \in C,\ \ni\ s=a+bi$
Seventh case: $s \in C,\ \ni\ s=-a-bi$
Eighth case: $s \in C,\ \ni\ s=-a+bi$

Treating the three cases above like the fifth case, we can prove that there are no roots of these types. Therefore, Eq. (A3) has only real negative roots like $s=-\alpha_p\nu_n^2$, $n=1, 2, 3,\ldots$.Now, to analyse the multiplicity of these roots, we return to Eq. (A6); if a root's multiplicity is greater than 1, there may also be roots of the successive derivatives of this equation. So, taking the derivative of both sides of Eq. (A6) relative to s,

$$\sum_{j=1}^{\infty}\frac{-s}{\left(s+zj^2\right)^2}+\sum_{j=1}^{\infty}\frac{1}{s+zj^2}=0$$

or,

$$\sum_{j=1}^{\infty}\frac{zj^2}{\left(s+zj^2\right)^2}=0$$

the left side of this equation is always greater than zero for s being a real number, either the multiplicity is one.

2. Roots of Eq. (A4): Initially, using Eqs. (39), (40) and (58), we put Eq. (A4) in the form:

$$I_0(\lambda R)-\frac{\gamma}{\chi s}\left[\frac{\omega}{1+\delta s\sum_{j=1}^{\infty}\frac{1}{s+zj^2}}-1\right]I_2(\lambda R)=0 \quad \text{(A7)}$$

$s=0$ is a zero of this equation.
Now, from Eq. (A7),

$$\chi s I_0(\lambda R)+\gamma I_2(\lambda R)=\frac{\gamma\omega I_2(\lambda R)}{\left(1+\delta s\sum_{j=1}^{\infty}\frac{1}{s+zj^2}\right)} \quad \text{(A8)}$$

or

$$\left(1+\delta s\sum_{j=1}^{\infty}\frac{1}{s+zj^2}\right)\left(\frac{\chi s I_0(\lambda R)}{\gamma I_2(\lambda R)}+1\right)=\omega \quad \text{(A9)}$$

First case: $s \in R_+^* \Rightarrow$ Eq. (A9) will have no roots, since $\omega \leq 1$ and the left-hand side of the equation is always greater than 1.
Second case: $s \in R_-^*$; let $s=-\alpha\tau^2/\chi$, then, from Eqs. (A9) and (A4) we have

$$\left\{1-\frac{\delta\alpha\tau^2}{\chi}\sum_{j=1}^{\infty}\frac{1}{zj^2-\frac{\alpha\tau^2}{\chi}}\right\}\left\{\frac{\alpha\tau^2 J_0(\tau R)}{\gamma J_2(\tau R)}+1\right\}=\omega \quad \text{(A10)}$$

when $\alpha\tau^2/\chi$ varies from zj^2 to $z(j+1)^2$; $j=1, 2, 3,\ldots$, the first brackets in the left-hand side of the above equation varies from $+\infty$ to $-\infty$; also, when passing through the zeros of $J_2(\tau R)$, the second brackets in the left-hand side varies from $+\infty$ to $-\infty$. Therefore, we may expect infinite zeros for Eq. (A10) at $s=-\alpha\tau_n^2/\chi$, $n=1, 2, 3,\ldots$
Third case: $s \in I_+,\ \ni\ s=bi;\ \ b>0$; then we may write Eq. (A9) in the form:

$$\left(1+\delta\sum_{j=1}^{\infty}\frac{bi}{bi+zj^2}\right)\left(sQ(\lambda)+1\right)=\omega, \quad \text{(A11)}$$

where $Q(\lambda)$ is defined as:

$$Q(\lambda)\equiv\frac{\chi I_0(\lambda R)}{\gamma I_2(\lambda R)} \quad \text{(A12)}$$

Now, multiplying by the complex conjugate in the series of the first parenthesis in the left-hand side of Eq. (A11),

$$\left(1+\delta\sum_{j=1}^{\infty}\frac{bi\,zj^2+b^2}{b^2+\left(zj^2\right)^2}\right)\left(sQ(\lambda)+1\right)=\omega, \quad \text{(A13)}$$

the expression above can also be written in the general form:

$$(1+c+di)\left(sQ(\lambda)+1\right)=\omega \quad \text{(A14)}$$

where c and d are positive real numbers, representing the results of the series in the first parenthesis, left-hand side; therefore,

$$sQ(\lambda)=\frac{\omega}{1+c+di}-1=\frac{\omega(1+c-di)}{(1+c)^2+d^2}-1 \quad \text{(A15)}$$

or

$$sQ(\lambda)=\frac{\omega(1+c)}{(1+c)^2+d^2}-1-\frac{di}{(1+c)^2+d^2}$$

Consequently, if Eq. (A4) has roots of the type $s=bi$, the following necessary conditions can be established from above:

$$\Longrightarrow \mathrm{Re}\{sQ(\lambda)\} < 0 \qquad \mathrm{Im}\{sQ(\lambda)\} < 0$$

$$\left|\mathrm{Re}\{sQ(\lambda)\}\right| < 1 \qquad \left|\mathrm{Im}\{sQ(\lambda)\}\right| < 1$$

where $\mathrm{Re}\{sQ(\lambda)\}$ and $\mathrm{Im}\{sQ(\lambda)\}$ are the real and imaginary parts of $sQ(\lambda)$, respectively.

$$\delta\sum_{j=1}^{\infty}\frac{zj^2}{\left(s+zj^2\right)^2} = -\omega\left[\frac{\chi s I_0(\lambda R)}{\gamma I_2(\lambda R)}+1\right]^{-2} \times \frac{2\gamma\chi I_2(\lambda R)I_0(\lambda R) - \chi\gamma I_1^2(\lambda R)}{\left[\gamma I_2(\lambda R)\right]^2} \tag{A16}$$

Also, substituting Eq. (55) in the above equation and following with algebraics,

$$\delta\sum_{j=1}^{\infty}\frac{zj^2}{\left(s+zj^2\right)^2} = -\omega\left[\frac{\chi s I_0(\lambda R)}{\gamma I_2(\lambda R)}+1\right]^{-2} \times \frac{2\gamma\chi I_2(\lambda R)I_0(\lambda R)\left[1+\left(\frac{\lambda R}{2}\right)^2\right] - \left(\frac{\lambda R}{2}\right)^2\chi\gamma\left[I_2^2(\lambda R)+I_0^2(\lambda R)\right]}{\left[\gamma I_2(\lambda R)\right]^2}$$

Taking $\lim_{s\to -\alpha\tau_n^2/\chi}$ in the above equation, results:

$$\delta\sum_{j=1}^{\infty}\frac{zj^2}{\left(zj^2-\frac{\alpha\tau_n^2}{\chi}\right)^2} = -\omega\left[\frac{\alpha\tau_n^2 J_0(\tau_n R)}{\gamma J_2(\tau_n R)}+1\right]^{-2} \times \frac{-2\gamma\chi J_2(\tau_n R)J_0(\tau_n R)\left[1-\left(\frac{\tau_n R}{2}\right)^2\right] + \left(\frac{\tau_n R}{2}\right)^2\chi\gamma\left[J_2^2(\tau_n R)+J_0^2(\tau_n R)\right]}{\left(\gamma J_2(\lambda R)\right)^2}$$

Also, for the remaining cases, the necessary conditions that can be established are:

Fourth case: $s = -bi$;

$$\Longrightarrow \mathrm{Re}\{sQ(\lambda)\} < 0 \qquad \mathrm{Im}\{sQ(\lambda)\} > 0$$

$$\left|\mathrm{Re}\{sQ(\lambda)\}\right| < 1 \qquad \left|\mathrm{Im}\{sQ(\lambda)\}\right| < 1$$

Fifth case: $s = a + bi \Rightarrow$ Idem to the third case.

Sixth case: $s = -a + bi \Longrightarrow \mathrm{Im}\{sQ(\lambda)\} < 0$

Seventh case: $s = a - bi \Rightarrow$ Idem to the fourth case.

Eighth case: $s = -a - bi \Longrightarrow \mathrm{Im}\{sQ(\lambda)\} > 0$

The Bessel functions for complex arguments are complex numbers. These, by contrast with trigonometric functions, cannot be separated into real and imaginary parts expressed in terms of known functions [22]; therefore, we have realized an extensive numerical study for the $sQ(\lambda)$ of the third to the eight case listed above, and verified that the necessary conditions refering to the signal of the imaginary parts are not satisfied. So, there are no roots like these for Eq. (A4).

In conclusion, Eq. (A4) has only real negative roots at $s = -\alpha\tau_n^2/\chi$, $n = 1, 2, 3\ldots$ and a root at $s = 0$.

Now, to analyze the multiplicity of these roots we first put the second parenthesis in the left-hand side of Eq. (A9) in the denominator of the right-hand side, and take the derivative of the resulting expression relative to s; second, after some manipulation, employing the recurrence relations of Bessel functions [12], it results in:

The right-hand side of the equation above will be always negative for $\tau_n R \geq 2 \Rightarrow$ multiplicity = 1 for $\tau_n R \geq 2$.

For the interval $0 < \tau_n R < 2$, we return to Eq. (A16) and apply $\lim_{s\to -\alpha\tau_n^2/\chi}$:

$$\delta\sum_{j=1}^{\infty}\frac{zj^2}{\left(zj^2-\frac{\alpha\tau_n^2}{\chi}\right)^2} = -\omega\left[\frac{\alpha\tau_n^2 J_0(\tau_n R)}{\gamma J_2(\tau_n R)}+1\right]^{-2} \times \frac{\gamma\chi\left[J_1^2(\tau_n R) - 2J_2(\tau_n R)J_0(\tau_n R)\right]}{\left[\gamma J_2(\tau_n R)\right]^2}$$

and since $J_1^2(\tau_n R) - 2J_2(\tau_n R)J_0(\tau_n R) > 0$, $\forall\, \tau_n R \in (0, 2)$ the right-hand side is always negative; therefore, Eq. (A16) will have no roots of the type $s = -\alpha\tau_n^2/\chi \Rightarrow$ multiplicity of the roots $s = -\alpha\tau_n^2/\chi$ of Eq. (A4) is one. The same can be demonstrated for $s = 0$.

Appendix B. Lumped Capacity Model [6]

The main simplifying hypothesis of this model is likewise the distributed parameter model (DP), except that:

- the fluid temperature is uniform over the pipe cross section;
- the eddy thermal diffusivity of the fluid is included in the model by means of a wall heat transfer coefficient, h_w.

B.1. Governing equations

In a similar manner that Eqs. (1)–(3), the particle and fluid energy balance respectively yields:

$$\frac{1}{\alpha_p}\frac{\partial T_p(\xi,t)}{\partial t}=\frac{\partial^2 T_p(\xi,t)}{\partial \xi^2}+\frac{2}{\xi}\frac{\partial^2 T_p(\xi,t)}{\partial \xi} \tag{B1}$$

$$\frac{u_f\rho_f C_f}{u_p}\frac{dT_f(t)}{dt} = \frac{h_w A_w}{V}(T_w - T_f(t)) - \frac{h_p n_v A_p}{V}\big(T_f(t) - T_{ps}(t)\big) \tag{B2}$$

The system formed by the above equations is subjected to the following boundary conditions:

$$\xi = R_p,\ t>0: \qquad T_p = T_{ps}(t) \tag{B3}$$

$$\xi = 0,\ t>0: \qquad T_p = \text{finite}, \tag{B4}$$

and the initial conditions,

$$t=0,\ 0<\xi<R_p: \qquad T_p = T_{pi} \tag{B5}$$

$$t=0,: \qquad T_f = T_{fi}, \tag{B6}$$

and also the additional condition:

$$\xi = R_p,\ t>0: \qquad -k_p\frac{\partial T_p}{\partial \xi} = h_p\big(T_{ps}(t)-T_f\big)+h_r\big(T_{ps}(t)-T_w\big) \tag{B7}$$

B.2. Solution of the model

The solution of this model (LP) follows analogously to the solution of the distributed parameter model (DP). Details on the development are given apart [6]. The resulting expressions are:

$$T_f(t) = T_w - \sum_{n=1}^{\infty}\exp\Big(-\alpha_p\sigma_n^2 t\Big)\frac{L(\sigma_n)}{\alpha_p\sigma_n^2}, \tag{B8}$$

$$T_{ps}(t) = T_w - \frac{1}{\gamma}\sum_{n=1}^{\infty}\exp\Big(-\alpha_p\sigma_n^2 t\Big)\frac{\Delta-\chi\alpha_p\sigma_n^2}{\alpha_p\sigma_n^2}L(\sigma_n) \tag{B9}$$

$$\begin{aligned}T_p(\xi,t) = {}& \phi(t)T_{pi} + \frac{2R_p}{\pi\xi}\sum_{j=1}^{\infty}\frac{(-1)^j}{j}\\ &\times\sin\left(\frac{j\pi\xi}{R_p}\right)\left\{\phi(0)T_{pi}\exp\left[-\left(\frac{j\pi}{R_p}\right)^2\alpha_p t\right]\right.\\ &+\frac{1}{\gamma}\sum_{n=1}^{\infty}\Big(\Delta-\chi\alpha_p\sigma_n^2\Big)L(\sigma_n)\\ &\times\left\{\exp\Big(-\alpha_p\sigma_n^2 t\Big)-\exp\left[-\left(\frac{j\pi}{R_p}\right)^2\alpha_p t\right]\right\}\\ &\left.\times\frac{1}{\alpha_p\left(\frac{j\pi}{R_p}\right)^2-\alpha_p\sigma_n^2}\right\}+T_{pi}\end{aligned} \tag{B10}$$

where

$$\begin{aligned}L(\sigma_n) = {}& \left\{-\chi\alpha_p\sigma_n^2 T_{fi}+\varphi T_w+\gamma T_{pi}\right.\\ &\times\left[1-\frac{2(\omega-\eta)}{2+\delta\big(\sigma_n R_p\cot(\sigma_n R_p)-1\big)}\right]\Bigg\}\Big/\Bigg\{\chi\\ &\left.+\frac{\omega\gamma\delta R_p\sigma_n}{\alpha_p\sigma_n}\,\frac{R_p\Big(1+\cot^2\big(\sigma_n R_p\big)\Big)-\cot\big(\sigma_n R_p\big)}{\big[2+\delta\big(\sigma_n R_p\cot(\sigma_n R_p)-1\big)\big]^2}\right\}\end{aligned} \tag{B11}$$

$\pm\sigma_n,\ n=1,\ 2,\ldots,$ are the roots of:

$$\Delta-\chi\alpha_p\sigma^2-\frac{2\omega\gamma}{2+\delta\big(\sigma R_p\cot(\sigma R_p)-1\big)}=0 \tag{B12}$$

and $\phi(t)$ is given by Eq. (18).

The mean temperature of the particle at time t, is obtained by integration of Eq. (B10) in the particle volume:

$$\begin{aligned}\bar{T}_p(t) = {}& \phi(t)T_{pi}-\frac{6}{\pi^2}\sum_{j=1}^{\infty}\frac{1}{j^2}\left\{\phi(0)T_{pi}\exp\left[-\left(\frac{j\pi}{R_p}\right)^2\alpha_p t\right]\right.\\ &+\frac{1}{\gamma}\sum_{n=1}^{\infty}\Big(\Delta-\chi\alpha_p\sigma_n^2\Big)L(\sigma_n)\times\left\{\exp\Big(-\alpha_p\sigma_n^2 t\Big)\right.\\ &\left.\left.-\exp\left[-\left(\frac{j\pi}{R_p}\right)^2\alpha_p t\right]\right\}\frac{1}{\alpha_p\big(j\pi/R_p\big)^2-\alpha_p\sigma_n^2}\right\}+T_{pi}\end{aligned} \tag{B13}$$

References

[1] L. Farbar, M.J. Morley, Heat transfer to flowing gas–solid mixtures in a circular tube, Industrial and Engineering Chemistry 49 (7) (1957) 1143–1150.

[2] C.L. Tien, Heat transfer by a turbulently flowing fluid–solid mixture in a pipe, Trans. ASME Journal of Heat Transfer C83 (1961) 183–188.

[3] S. Matsumoto, A. Takahashi, M. Susuki, S. Maeda, Gas temperature distributions and eddy diffusivity of heat in gaseous suspension flow, Journal of Chemical Engineering of Japan 12 (3) (1979) 183–189.

[4] F.H. Azad, M.F. Modest, Combined radiation and convection in absorbing, emitting and anisotropically scattering gas–particulate tube flow, International Journal of Heat and Mass Transfer 24 (1981) 1681–1698.

[5] A.C.L. Lisbôa, Transferência de Calor em Leito de Arrasto de Xisto, M.Sc. thesis, COPPE, Federal University of Rio de Janeiro, Rio de Janeiro, RJ, 1987.

[6] S.L. Bertoli, Transferência de Calor Convectiva e Radiante em Leito de Arrasto, M.Sc. thesis, COPPE, Federal University of Rio de Janeiro, Rio de Janeiro, RJ, 1989.

[7] W.D. Munro, N.R. Amudson, Solid–fluid heat exchange in moving beds, Industrial and Engineering Chemistry 42 (8) (1950) 1481–1488.

[8] E.C. Titchmarsh, Theory of Functions, Oxford University Press, London, 1939, p. 268.

[9] C.W. Siegmund, W.D. Munro, N.R. Amudson, Two problems on moving beds, Industrial and Engineering Chemistry 48 (1) (1956) 43–50.

[10] C.M. Hackenberg, On the unsteady resistance of submerged spherical bodies, Ph.D. thesis, University of Florida, 1969.

[11] A.D. Wheeelon, in: Tables of Summable Series and Integrals Involving Bessel Functions, Holden-Day, San Francisco, 1968, p. 22.

[12] F.W.J. Oliver, Bessel functions of integer order, in: M. Abramowitz, I. Stegun (Eds.), Handbook of Mathematical Functions, Doover, New York, 1972, pp. 355–433.

[13] L.Y. Luke, Integrals of Bessel functions, in: M. Abramowitz, I. Stegun (Eds.), Handbook of Mathematical Functions, Dover, New York, 1972, pp. 479–494.

[14] C.R. Wylie, L.C. Barrett, Advanced Engineering Mathematics, 5th ed., McGraw-Hill, Singapore, 1985, p. 967.

[15] M. Jakob, Heat Transfer, Wiley, New York, 1949, p. 459.

[16] K. Kato, L. Onozawa, Y. Noguchi, Gas particle heat transfer in a dispersed bed, Journal of Chemical Engineering of Japan 16 (3) (1983) 178–182.

[17] M.A. Boothroyd, H. Haque, Experimental investigation of heat transfer in the entrance region of a heated duct conveying fine particles, Trans. Instn. Chem. Engrs 48 (1970) T109–T120.

[18] H. Tamehiro, R. Echigo, S. Hasegawa, Radiative heat transfer by flowing multiphase medium. Part III: an analysis on heat transfer of turbulent flow in a circular tube, International Journal of Heat and Mass Transfer 16 (1973) 1199–1213.

[19] C.L. Tien, Radiation properties of particulates, in: W.M. Rosenow, J.P. Hartnett, E.N. Ganic (Eds.), Handbook of Heat Transfer Fundamentals, 2nd ed., McGraw-Hill, New York, 1985, pp. 84–86 (Chapter 14).

[20] M.Q. Brewster, C.L. Tien, Radiative: dependent versus independent scattering, Trans. ASME, Journal of Heat Transfer 104 (1982) 573–579.

[21] S. deSoto, Coupled radiation, conduction and convection in entrance region flow, International Journal of Heat and Mass Transfer 11 (1968) 39–53.

[22] V.S. Arpacy, Conduction Heat Transfer, Addison-Wesley, Reading, 1966, p. 332.